

# Microwave dielectric properties of aluminum substituted $\text{Ca}_{0.61}\text{Nd}_{0.26}\text{TiO}_3$ ceramics

Hetuo CHEN,<sup>\*,\*\*</sup> Bin TANG,<sup>\*,\*\*,\*†</sup> Peng FAN,<sup>\*\*</sup> Shuxin DUAN,<sup>\*\*</sup>

Meng WEI,<sup>\*\*</sup> Ying YUAN,<sup>\*,\*\*</sup> and Shuren ZHANG<sup>\*,\*\*</sup>

<sup>\*</sup>National Engineering Research Center of Electromagnetic Radiation Control Materials, University of Electronic Science and Technology of China, Jianshe Road, Chengdu, 610054, People's Republic of China

<sup>\*\*</sup>State Key Laboratory of Electronic Thin Films and Integrated Devices, University of Electronic Science and Technology of China, Jianshe Road, Chengdu, 610054, People's Republic of China

According to the solid state reaction routine,  $\text{Ca}_{0.61}\text{Nd}_{0.26}\text{Ti}_{1-x}\text{Al}_{4x/3}\text{O}_3$  ( $x = 0, 0.05, 0.1, 0.15, 0.2$ ) ceramics were synthesized and their microwave dielectric properties were determined. The X-ray diffraction results showed a single perovskite phase (JCPDS Card No. 01-082-0229) for  $0 \leq x \leq 0.1$ . Dielectric constant ( $\epsilon_r$ ) decreased from 102.8 to 72.24, the  $Q \times f$  value almost doubled, from 8560 to 15437 GHz, and the temperature coefficient of resonant frequency ( $\tau_f$ ) dropped from +247 to +155 ppm/°C. Then the X-ray diffraction patterns showed the appearance of secondary phase that degraded microwave dielectric properties of the system rapidly. At last, a ceramic possessing microwave dielectric properties of  $\epsilon_r = 72.24$ ,  $Q \times f = 15437$  GHz and  $\tau_f = +155$  ppm/°C could be obtained when sintered at 1400°C for 2 h in air,  $x = 0.1$ .

©2016 The Ceramic Society of Japan. All rights reserved.

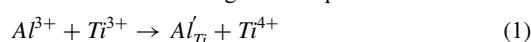
Key-words : Electroceramics, Microstructure, X-ray techniques

[Received January 4, 2016; Accepted May 22, 2016]

## 1. Introduction

The rapid growth of wireless communication applications, such as, Wi-Fi and RFID, has been placing increasing requests on the performance of microwave dielectric materials at the microwave range.<sup>1)</sup> Higher  $\epsilon_r$  for minimization of application dimension, higher  $Q \times f$  value for better signal selection, and near zero  $\tau_f$  for the stability of the dielectric devices regarding temperature are the three standards for these materials design.<sup>2)</sup>

One kind of these ceramics,  $\text{Ca}_{0.61}\text{Nd}_{0.26}\text{TiO}_3$  ceramic ( $\epsilon_r \sim 100$ ), has been extensively investigated for its high dielectric constant and high  $Q \times f$  value, however, its large positive  $\tau_f$  value of +247 ppm/°C always hindered its wide use.<sup>3)</sup> Until now, methods like ionic substitution or combining two phases with opposite temperature coefficient at resonant frequency have been reported to tailoring its properties.<sup>3),4)</sup> For example, bismuth substitution for neodymium can enhance the dielectric constant and quality factor but result in a higher temperature coefficient of resonant frequency value.<sup>4)</sup> Another example,  $0.55\text{Ca}_{0.61}\text{Nd}_{0.26}\text{TiO}_3-0.45\text{Li}_{1/2}\text{Nd}_{1/2}\text{TiO}_3$  composition showed properties of  $\epsilon_r \sim 101$  and  $Q \times f \sim 5300$  GHz, and  $\tau_f \sim +13$  ppm/°C.<sup>3)</sup> However, in practical manufacture, it was troublesome to synthesis two phases separately. Another method of doping  $\text{Al}_2\text{O}_3$  can effectively improve  $Q \times f$  value and drive  $\tau_f$  towards zero in  $\text{Ba}_{6-3x}\text{Nd}_{8+2x}\text{Ti}_{18}\text{O}_{54}$  ceramics and it has already been reported to take the place of titanium site according to the equation below:



in which  $\text{Al}^{3+}$  restrained  $\text{Ti}^{4+}$  reduction.<sup>5)-8)</sup>

Based on the statements above, in this paper,  $\text{Ca}_{0.61}\text{Nd}_{0.26}\text{Ti}_{1-x}\text{Al}_{4x/3}\text{O}_3$  ceramics were synthesized. The effects of aluminum substitution upon microstructure and microwave dielectric prop-

erties were also investigated.

## 2. Experimental procedure

The ceramics were fabricated by solid-state reaction routine according to the formula of  $\text{Ca}_{0.61}\text{Nd}_{0.26}\text{Ti}_{1-x}\text{Al}_{4x/3}\text{O}_3$  ( $x = 0, 0.05, 0.1, 0.15, 0.2$ ). The high-purity ( $\geq 99\%$ ) starting materials of  $\text{CaCO}_3$ ,  $\text{Nd}_2\text{O}_3$ ,  $\text{TiO}_2$  and  $\text{Al}_2\text{O}_3$  were ball-milled in nylon jars with zirconia balls and deionized water for 12 h. Then these powders were calcined at 1130°C for 5 h. The calcined powders were produced with 5wt % PVA in the size of 15 mm in diameter and 7 mm in thickness under the pressure of 250 kg/cm<sup>2</sup>. At last, the samples were preheated at 600°C for 2 h to remove the organic binder, and sintered at 1350–1425°C for 2 h.

Densities of sintered samples were measured by Archimedes method. The phase of the sintered samples was identified by the X-ray diffraction (XRD). Microwave dielectric characteristics were examined by the Hakki-Coleman dielectric resonator method in the TE<sub>011</sub> mode using a network analyzer at frequency around 3–5 GHz. The  $\tau_f$  values of sintered samples were determined by the equation as following:

$$\tau_f = \frac{f_{t_2} - f_{t_1}}{f_{t_1} \times (t_2 - t_1)} \times 10^6 \quad (2)$$

where  $f_{t_1}$  and  $f_{t_2}$  were the resonant frequencies at the temperature of  $t_1$  (ordinary temperature) and  $t_2 = 85^\circ\text{C}$  respectively.

## 3. Result and discussion

Figure 1 showed the X-ray diffraction results of  $\text{Ca}_{0.61}\text{Nd}_{0.26}\text{Ti}_{1-x}\text{Al}_{4x/3}\text{O}_3$  ( $x = 0, 0.05, 0.1, 0.15, 0.2$ ) ceramics sintered at 1400°C for 2 h. For  $0 \leq x \leq 0.1$ , the results showed a single perovskite phase (JCPDS Card No. 01-082-0229). In order to check if it was the result of substitution, here we calculated crystal parameters according to the XRD data and the results were depicted in Fig. 2. The decreasing parameters indicated that

<sup>†</sup> Corresponding author: B. Tang; E-mail: tangbin@uestc.edu.cn

B-site  $\text{Ti}^{4+}$  (0.0605 nm) was replaced by  $\text{Al}^{3+}$  (0.0505 nm) and  $\text{Ca}_{0.61}\text{Nd}_{0.26}(\text{Ti},\text{Al})\text{O}_3$  solid solution was formed.<sup>7)</sup> For  $0.15 \leq x \leq 0.2$ , a  $(\text{Ca},\text{Nd})_2(\text{Ti},\text{Al})_2\text{O}_{6-\alpha}$  (JCPDS Card No. 00-042-0002) secondary phase appeared rather than  $\text{Al}_2\text{O}_3$  phase. Its appearance determined that the solid solution limit was around 0.1.<sup>7)</sup>

Figures 3(a)–3(e) were microstructure images of  $\text{Ca}_{0.61}\text{Nd}_{0.26}\text{Ti}_{1-x}\text{Al}_{4x/3}\text{O}_3$  ( $x = 0, 0.05, 0.1, 0.15, 0.2$ ) ceramics sintered at  $1400^\circ\text{C}$  and (f) was an enlarged part of (e) to clearly view its surface morphology. As  $x$  value growing from 0 to 0.2 the grain size dropped evidently. This phenomenon proved that  $\text{Al}_2\text{O}_3$  may degrade grain size of this ceramic system. In (d) and (e), a kind of cubic grain, with a hole in the middle marked by “S”, was clearly denoted by “+” in (f). To make sure the phase element constitution, element ratio data of the energy dispersive X-ray analysis (EDS) were collected. Here we took spots A, B and spots denoted by “+” for the secondary phase and by “x” for the main phase in Figs. 3(a), 3(c) and 3(f) separately for example and

listed their data in Table 1. The oxygen ratio difference between A and B inferred that titanium reduction was tackled by aluminum substitution.<sup>6),7)</sup> The element ratio results of “+” and “x” confirmed the perovskite phase and  $(\text{Ca},\text{Nd})_2(\text{Ti},\text{Al})_2\text{O}_{6-\alpha}$  phase shown in XRD results.

Figure 4(a) showed the bulk densities of the specimens. When temperature increased from  $1350$  to  $1400^\circ\text{C}$ , the density showed a growing trend. Then the density decreased when temperature was further increased to  $1425^\circ\text{C}$ , which inferred that  $1400^\circ\text{C}$  was the optimal sintering temperature. Also, as  $x$  value increasing from 0 to 0.2, the density of the well sintered ceramic kept decreasing. This trend was consistent with microstructure variation of Figs. 3(a)–3(e).

Figures 4(b)–4(d) showed microwave dielectric properties data of  $\text{Ca}_{0.61}\text{Nd}_{0.26}\text{Ti}_{1-x}\text{Al}_{4x/3}\text{O}_3$  ( $x = 0, 0.05, 0.1, 0.15, 0.2$ ) ceramics. As reported, there were many factors that could control properties of the system and it was always hard to tell which was the most important.<sup>9)</sup> Based on the examination technique, for example, XRD and SEM, we can figure out that the secondary phase would play a key role in the declination of the microwave dielectric properties of the system for  $0.15 \leq x \leq 0.2$ .<sup>10)</sup>

The dielectric constant decreased from 102.8 to 47.96 according to the increase of  $x$  value. While in this study  $\text{Ti}^{4+}$  ( $2.94 \text{ \AA}$ ) was replaced by  $\text{Al}^{3+}$  ( $0.78 \text{ \AA}$ ) with lower ionic polarizability, the declining apparent density in Fig. 4(a), dropping grain size in Figs. 3(a)–3(e) and the secondary phase made it clear that dielectric constant was controlled by them.<sup>11)</sup>

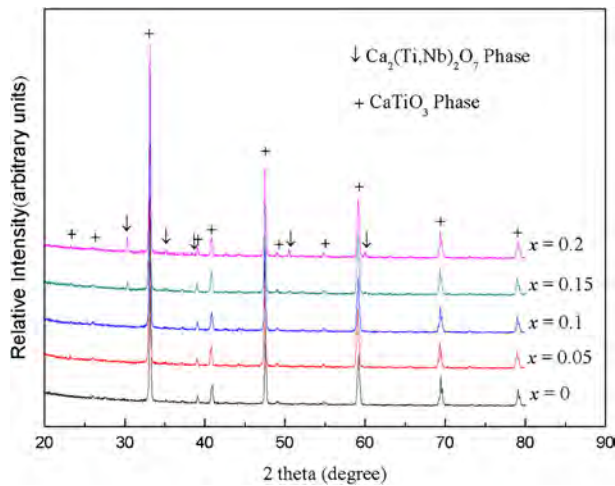


Fig. 1. The X-ray diffraction patterns of  $\text{Ca}_{0.61}\text{Nd}_{0.26}\text{Ti}_{1-x}\text{Al}_{4x/3}\text{O}_3$  ( $0 \leq x \leq 0.2$ ) ceramics sintered at  $1400^\circ\text{C}$  for 2 h.

Table 1. EDX results of spot A, B, “+” and “x” marked in Figs. 3(a), 3(b) and 3(f)

Spot	Atom (%)				
	Ca	Nd	Ti	Al	O
A	15.22	5.98	27.21	—	51.59
B	12.95	4.82	18.78	2.15	61.3
+	14.12	6.01	14.96	5.11	59.8
x	12.53	4.31	16.42	4.11	62.81

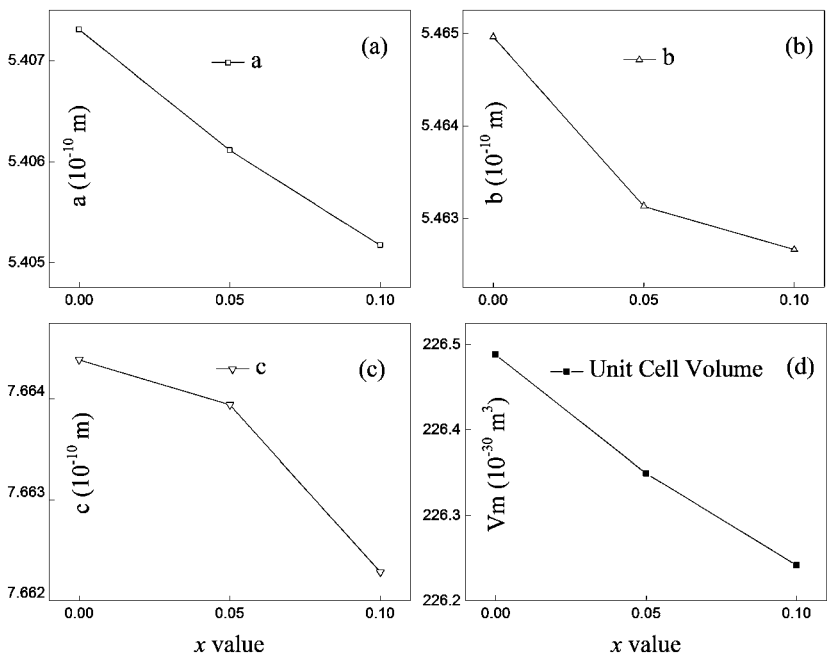


Fig. 2. Crystal parameters of  $\text{Ca}_{0.61}\text{Nd}_{0.26}\text{Ti}_{1-x}\text{Al}_{4x/3}\text{O}_3$  ( $0 \leq x \leq 0.1$ ) ceramics as a function of  $x$  value.

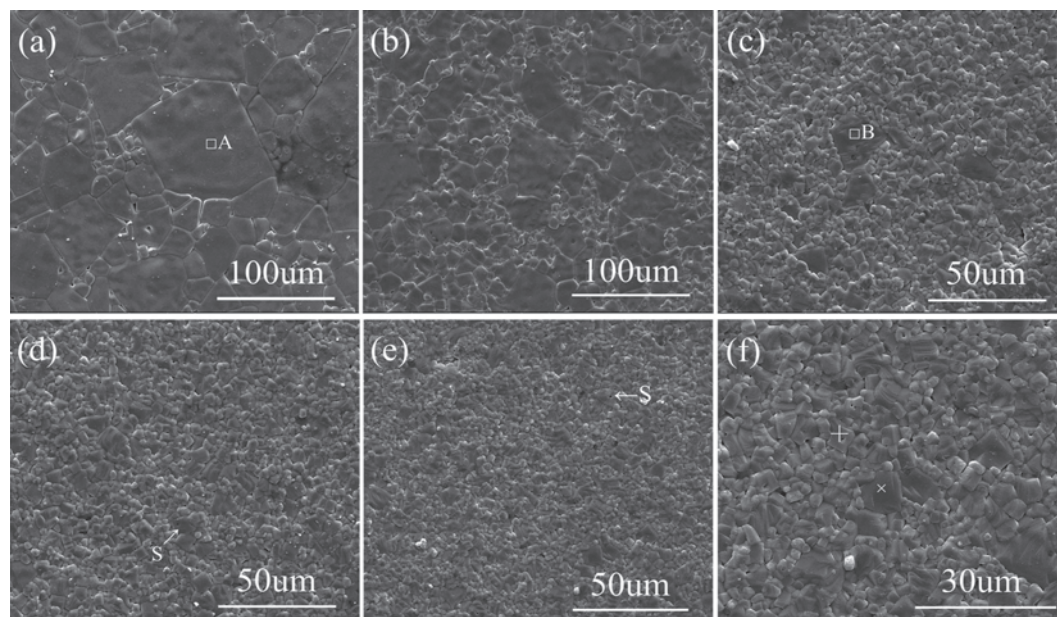


Fig. 3. (a)–(e): SEM images of  $\text{Ca}_{0.61}\text{Nd}_{0.26}\text{Ti}_{1-x}\text{Al}_{4x/3}\text{O}_3$  ( $0 \leq x \leq 0.2$ ) ceramics sintered at  $1400^\circ\text{C}$ ; Fig. 3(f) showed an enlarged part of Fig. 3(e).

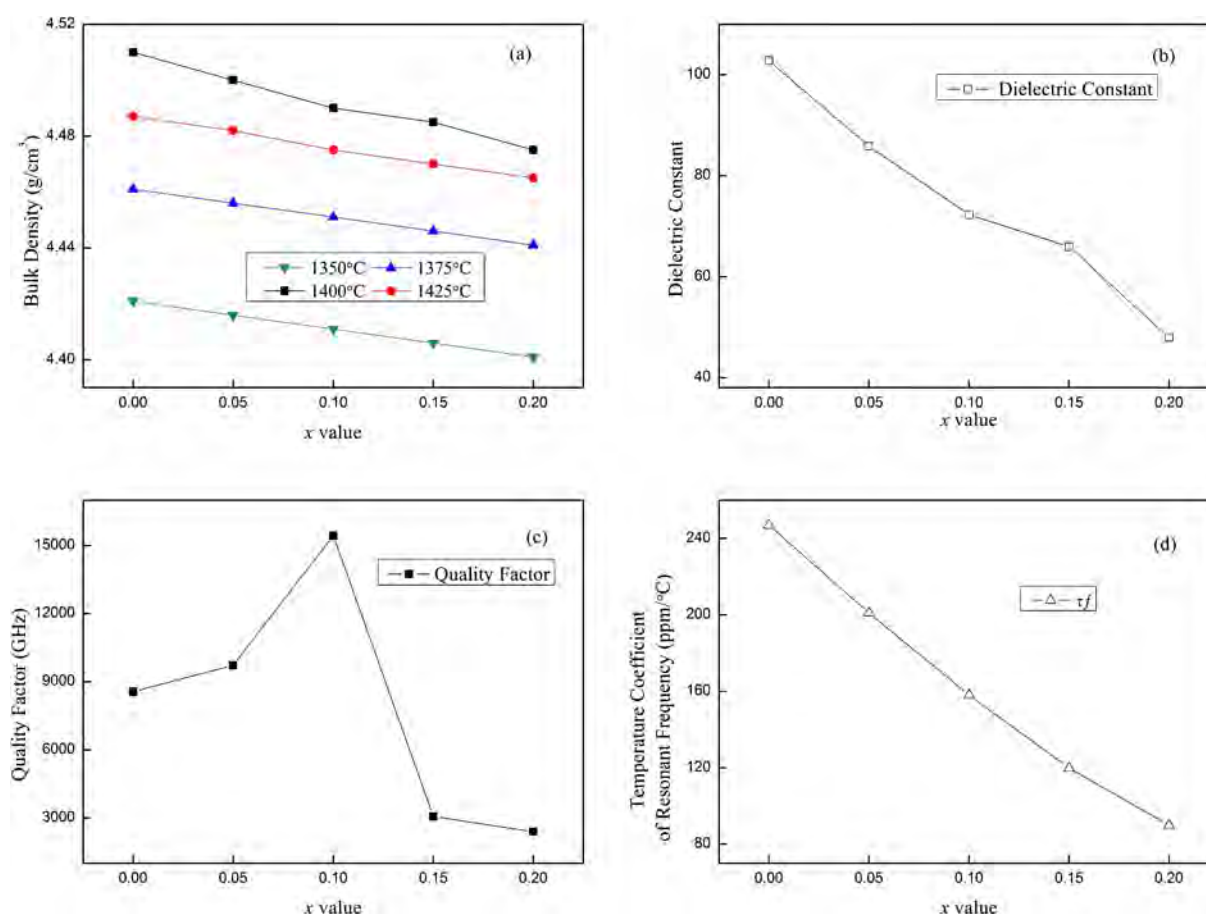


Fig. 4. (a)–(d): Bulk density and microwave dielectric properties of  $\text{Ca}_{0.61}\text{Nd}_{0.26}\text{Ti}_{1-x}\text{Al}_{4x/3}\text{O}_3$  ( $0 \leq x \leq 0.2$ ) ceramics as a function of  $x$  value.

The  $Q \times f$  increased sharply from 8560 to 15437 GHz for  $x = 0.1$ , and then decreased to 2390 GHz. The rapid growth may be resulted from the substitution mechanism as previous reports: at

high temperature, titanium reduction occurred which was the reason why the  $Q \times f$  value was lower than some reports and aluminum substitution [shown in Eq. (1)] would conduct more

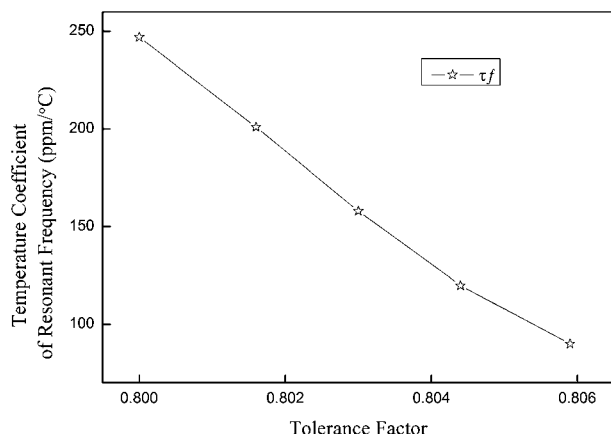


Fig. 5. Temperature coefficients of resonant frequency data of  $\text{Ca}_{0.61}\text{Nd}_{0.26}\text{Ti}_{1-x}\text{Al}_{4x/3}\text{O}_3$  ( $0 \leq x \leq 0.2$ ) ceramics as a function of tolerance factor.

oxygen vacancies that would restrain titanium reduction and then  $Q \times f$  value of the samples increased.<sup>2),5)-8),12)</sup> The EDS data in Table 1 confirmed this mechanism derivation. Because of the growing  $Q \times f$  value in  $0 \leq x \leq 0.1$  with declined grain size, for the declination of the  $Q \times f$  value of  $0.15 \leq x \leq 0.2$ , high tangent loss secondary phase probably played a key role.

Temperature coefficient decreased from +247 to +90 ppm/°C when  $x$  value increased from 0 to 0.2. The fact  $\text{Al}^{3+}$  replacing  $\text{Ti}^{4+}$  site was proved by the changing lattice parameters.<sup>5)-9)</sup> The substituted samples' octahedra must be distorted at a different degree and the degree of octahedral distortion was always evaluated by the tolerance factor calculated by the following equation:<sup>13)</sup>

$$t = \frac{0.61R_{\text{Ca}^{2+}} + 0.26R_{\text{Nd}^{3+}} + R_{\text{O}^{2-}}}{\sqrt{2}[(1-x)R_{\text{Ti}^{4+}} + \frac{4x}{3}R_{\text{Al}^{3+}} + R_{\text{O}^{2-}}]} \quad (3)$$

Figure 5 showed the relationship between the temperature coefficient of resonant frequency and the tolerance factor. With increasing  $x$  value, the increasing tolerance factor implied a decreasing temperature coefficient of resonant frequency.<sup>13)</sup> For the samples with secondary phase, the temperature coefficient at resonant frequency kept dropping still and therefore we believed that the secondary phase could also help to tailor  $\tau_f$  value.

## 4. Conclusions

The effects of aluminum substitution upon microstructure and microwave dielectric properties of  $\text{Ca}_{0.61}\text{Nd}_{0.26}\text{Ti}_{1-x}\text{Al}_{4x/3}\text{O}_3$  ( $0 \leq x \leq 0.2$ ) ceramics have been investigated in the study.  $\text{Al}^{3+}$  would take the place of  $\text{Ti}^{4+}$  which was the reason why  $Q \times f$  value of the system increased rapidly and  $\tau_f$  value decreased. The substituted ceramics possessed smaller grain size, higher pore ratio that influenced the dielectric constant of the ceramics. Typically, excellent microwave dielectric properties of  $\epsilon_r = 72.24$ ,  $Q \times f = 15473$  GHz and  $\tau_f = +155$  ppm/°C could be obtained when  $x = 0.1$  sintered at 1400°C for 2 h in air.

**Acknowledgements** This work is supported by the Open Foundation of National Engineering Research Center of Electromagnetic Radiation Control Materials (ZYGX2014K003-6) and the National Natural Science Foundation of China (Grant No. 51402039).

**Notes** The authors declare no competing financial interest.

## Reference

- 1) M. T. Sebastian, Dielectric materials for wireless communications, Elsevier Publishers, Oxford (2008) pp. 161–204.
- 2) H. T. Chen, B. Tang, S. X. Duan, H. Yang, Y. X. Li, H. Li and S. R. Zhang, *J. Electron. Mater.*, **44**, 1081–1087 (2015).
- 3) H. L. Chen and C. L. Huang, *Jpn. J. Appl. Phys.*, **41**, 5650–5653 (2002).
- 4) J. Qu, F. Liu, C. Yuan, X. Liu and G. H. Chen, *Mater. Lett.*, **159**, 436–438 (2015).
- 5) X. G. Yao, H. X. Lin, W. Chen and L. Luo, *Ceram. Soc.*, **38**, 3011–3016 (2012).
- 6) A. Templeton, X. R. Wang, S. J. Penn, S. J. Webb, L. F. Cohen and N. M. Alford, *J. Am. Ceram. Soc.*, **83**, 95–100 (2000).
- 7) H. T. Chen, B. Tang, A. Gao, S. Duan, H. Yang, Y. Li, H. Li and S. Zhang, *J. Mater. Sci.: Mater. Electron.*, **26**, 405–410 (2015).
- 8) H. T. Chen, B. Tang, Z. Xiong and S. R. Zhang, *Int. J. Appl. Ceram. Tec.*, **13**, 564–568 (2016).
- 9) B. Tang, S. Q. Yu, H. T. Chen, S. R. Zhang, and X. H. Zhou, *J. Alloys Comp.*, **551**, 463–467 (2013).
- 10) C. C. Li, X. Y. Wei, H. X. Yan and M. J. Reece, *J. Eur. Ceram. Soc.*, **32**, 4015–4020 (2012).
- 11) R. D. Shannon, *J. Appl. Phys.*, **73**, 348–365 (1993).
- 12) M. Yoshida, N. Hara, T. Takada and A. Seki, *Jpn. J. Appl. Phys.*, **36**, 6818–6823 (1997).
- 13) F. Zhao, Z. X. Yue, Y. C. Zhang, Z. L. Gui and L. T. Li, *J. Eur. Ceram. Soc.*, **25**, 3347–3352 (2005).